Adaptive Control of Magnetostrictive-Actuated Positioning Systems with Input Saturation

Zhi Li[1(✉)] and Chun-Yi Su[2]

[1] Department of Electrical Engineering, Eindhoven University of Technology, 5612AZ Eindhoven, Netherlands
zhi.li@tue.nl

[2] College of Automation Science and Engineering, South China University of Technology, Guangzhou 510641, China
cysu@scut.edu.cn

Abstract. Magnetostrictive actuators are high-force low-displacement actuators, which are profitably utilized in many engineering applications such as, high dynamic servo valves, micro/nano-positioning systems and optical systems. Nevertheless, magnetostrictive actuators are subject to hysteresis effects and input saturation, which lead poor system performances, e.g. inaccuracy and strong oscillations. To mitigate these effects, in this paper an adaptive controller with an anti-windup technique is developed. The anti-windup technique is particularly used for dealing with the input saturation effect. The simulation results demonstrate the effectiveness of the proposed controller.

Keywords: Input saturation · Hysteresis · Adaptive control · Anti-windup technique · Magnetostrictive actuators

1 Introduction

Magnetostrictive actuators exhibit dominant hysteresis behaviors between the input (current) and the output (displacement) [1]. Such nonlinearities limit the actuating precision and performance, and may cause undesirable inaccuracies or oscillations in the output, specifically when used in closed-loop control systems [2]. The common approach to compensate for the hysteretic behaviors is to construct its feedforward inverse compensator. However, this inverse compensation is open-loop based, which is vulnerable to the model uncertainty and system disturbance, etc. To overcome this disadvantage, the feedback control approaches are adopted, such as sliding mode control [3], adaptive backstepping control [4], neural network control [5], model predictive control [6], etc.

Apart from the hysteresis behaviors, the actuator saturation effect is also a common phenomenon appearing in the smart material based actuators. In practice, actuators are always subject to the magnitude limit. Thus, the applied control signal to the actuator should always be maintained within a certain range during the operation of the actuator. However, once the actuator reaches to its

N. Kubota et al. (Eds.): ICIRA 2016, Part I, LNAI 9834, pp. 635–645, 2016.
DOI: 10.1007/978-3-319-43506-0_55

saturation limit without being properly addressed, the performance of the actuator will be degraded. In the literature, approaches for dealing with the input saturation can be classified into two categories: the direct design method, where the saturation is considered in the construction of the Lyapunov function when synthesizing the designed controllers. The other category is the anti-windup design method [7,8], where a separate anti-windup block is implemented to deal with the limitation of the saturation. The advantage of the anti-windup technique is that it is independent of the controller design of the unconstrained system (without considering the input saturation) and therefore it is more feasible and easier to implement in practice. In this paper, an anti-windup control strategy combined with an adaptive controller is developed to address the input saturation and hysteresis nonlinearity in the magnetostrictive actuator. The simulations are studied to validate the effectiveness of the proposed control strategy.

2 Dynamic Modeling of the Magnetostrictive Actuated Systems

In [9], a dynamic model based on the principle of operation of the magnetostrictive actuator has been proposed, which comprehensively considers the electric, magnetic and mechanical domain as well as the interactions among them. The complete set of electric-magnetic-mechanical equations is as follows:

$$i(t) = i_a(t) + i_R(t) + i_H(t) \tag{1}$$

$$i_a(t) = \Phi_L(t)/L_A \tag{2}$$

$$i_R(t) = N\frac{\dot{\Phi}(t)}{R_0} \tag{3}$$

$$i_H(t) = \Pi[x] \tag{4}$$

$$\Phi(t) = \Phi_L(t) + \Phi_T(t). \tag{5}$$

$$\Phi_T(t) = T_{Mm}x(t) \tag{6}$$

$$m\ddot{x}(t) + b_s\dot{x}(t) + k_s x(t) = F_a(t) \tag{7}$$

$$F_a(t) = T_{em}i_a(t) \tag{8}$$

where $i(t)$ is the supplied current to the actuator; $i_H(t)$ denotes the hysteresis current loss, $\Pi[x]$ is a hysteresis operator which will be explained in the following development; i_R is the eddy current loss, with R_0 being the equivalent resistor of the eddy current effect, N denotes the number of turns of the solenoid; $i_a(t)$ is the actual applied current considering the hysteresis current loss and eddy current loss; $\Phi(t)$ is the magnetic flux flowing through the actuator; L_A denotes the equivalent inductor of the winding coils and $\Phi_L(t)$ is the magnetic flux flowing through the inductor L_A; $\Phi_T(t) = T_{Mm}x(t)$ is transformed from the mechanical side which is similar to the back-emf in piezoelectric actuator [10,11], T_{Mm} is

magnetomechanical transduction coefficient; m is the equivalent mass of the moving part, b_s is the equivalent damping coefficient and k_s is the equivalent stiffness of the preloaded spring; F_a denotes the applied force; $T_{em} = AE^H d_{33} N_a$ denotes the electromechanical transduction coefficient, where A is the cross section area of the magnetostrictive rod, E^H is the Young's modulus at constant value of magnetic field H, d_{33} is the slope of the strain versus the magnetic field, N_a denotes the number of turns of the solenoid per unit length.

By summarizing above equations, the general dynamic model of the magnetostrictive-actuated system can be written as:

$$m\ddot{x}(t) + b_s\dot{x}(t) + (k_s + \frac{T_{em}T_{Mm}}{L_a})x(t) = \frac{T_{em}}{L_a}\Phi(t) \tag{9}$$

$$NL_a\frac{\dot{\Phi}(t)}{R_0} + \Phi(t) - T_{Mm}x(t) = L_a(i(t) - \Pi[x](t)) \tag{10}$$

3 Adaptive Control Design for the Magnetostrictive System with Input Saturation

As mentioned in the introduction, the hysteresis nonlinearity and the input saturation degrade the tracking performance of the actuator and cause oscillations and even instabilities in the actuated systems. The existing controllers are designed either by keeping the control input not to reach the saturation limit or directly ignoring the saturation nonlinearity. In this section, an adaptive control strategy combined with an anti-windup technique is investigated for the purpose of improving the tracking performance of the system.

3.1 The Dynamic Model with Input Saturation

For the control purpose, the dynamic system in (9) and (10) is rewritten in the canonical form as

$$\dddot{x}(t) + \rho_2\ddot{x}(t) + \rho_1\dot{x}(t) + \rho_0 x(t) = b\Gamma[i](t) \tag{11}$$

where $\rho_2 = \frac{NL_a b_s + R_0 m}{NL_a m}$, $\rho_1 = \frac{NL_a k_s + NT_{em}T_{Mm} + R_0 b_s}{NL_a m}$, $\rho_0 = \frac{k_s R_0}{NL_a m}$, $b = \frac{R_0 T_{em}}{NL_a m}$. Because the displacement $x(t)$ can be represented as a function of supplied current $i(t)$, the term $i(t) - \Pi[x](t)$ in (10) can be defined as a new hysteresis nonlinearity $\Gamma[i](t)$

$$\Gamma[i](t) = u(t) = i(t) - \Pi[x](t) \tag{12}$$

Due to presence of the input saturation block, the input current $i(t)$ to the actuator becomes $i_{sat}(t) = sat_{\alpha,\beta}(i(t))$, where $sat_{\alpha,\beta}(i(t))$ is defined as

$$sat_{\alpha,\beta}(i(t)) = \begin{cases} \alpha, & \text{if } i(t) < \alpha \\ i(t), & \text{if } \alpha \le i(t) \le \beta \\ \beta, & \text{if } i(t) > \beta \end{cases}$$

Hence, the state space expression of the magnetostrictive-actuated dynamic system (11) can be expressed as

$$\begin{aligned}\dot{x}_1 &= x_2\\ \dot{x}_2 &= x_3\\ \dot{x}_3 &= -\rho_2 x_3 - \rho_1 x_2 - \rho_0 x_1 + bu(t)\end{aligned} \tag{13}$$

with

$$u(t) = \Gamma[sat_{\alpha,\beta}(i)](t) \tag{14}$$

3.2 Parameters Identification of the Magnetostrictive-Actuated Dynamic System in Absence of Input Saturation

From the model expression in (13) and (14), the dynamic model shows a cascading structure in which a nonlinear component, i.e. a hysteresis formulation $\Gamma[\cdot]$, is followed by a linear system. To identify this cascading structure, normalization should be conducted first. Without loss of generality, in this section, the dynamic part in (13) is normalized as follows

$$\begin{aligned}\dot{x}_1 &= x_2\\ \dot{x}_2 &= x_3\\ \dot{x}_3 &= -\rho_2 x_3 - \rho_1 x_2 - \rho_0 x_1 + \rho_0 u(t)\end{aligned} \tag{15}$$

with

$$u(t) = \Gamma_b[i](t) = \frac{b}{\rho_0}\Gamma[i](t) \tag{16}$$

Thus, the identification procedure is taken two steps as follows.
Step 1: Identification of the hysteresis component $\Gamma_b[i](t)$.
From experimental tests, hysteresis effects exhibited in the magnetostrictive actuator show asymmetric characteristics. To describe the asymmetric hysteresis behavior, an ASPI model [12] is employed in this paper. The numerical ASPI model is expressed as

$$\begin{aligned}\Gamma_b[i](t) &= P[i](t) + H[i](t)\\ &= P[i](t) + \Psi[i](t) + g(i)(t)\\ &= p_0 i(t) + \sum_{j=1}^{n} p_j F_{r_j}[i](t) + \sum_{j=1}^{M} q_j \Psi_{c_j}[i](t) + g(i)(t)\end{aligned} \tag{17}$$

where p_j denotes the weight of the play operator; $F_{r_j}[i](t)$ is the play operator, which is defined as

$$F_r[i](0) = f_r(i(0), 0) \tag{18}$$

$$F_r[i](t) = f_r(i(t), F_r[i](t_j)) \tag{19}$$

for $t_j < t \leq t_{j+1}, 0 \leq j \leq N-1$, with

$$f_r(i,w) = \max(i-r, \min(i+r, w)) \tag{20}$$

r_j in (17) denotes the threshold of the play operator, and n is the number of the play operators, q_j denotes the weight of the elementary shift operator, $\Psi_{c_j}[i](t)$ is the elementary shift operator, defined as

$$\Psi_c[i](0) = \psi_c(i(0), 0) \tag{21}$$

$$\Psi_c[i](t) = \psi_c(i(t), \psi_c[i](t_j)) \tag{22}$$

for $t_j < t \leq t_{j+1}, 0 \leq j \leq N-1$, with

$$\psi_c(i,w) = \max(ci, \min(i,w)) \tag{23}$$

c_j in (17) denotes the slope of the shift operator, and M is the number of the elementary shift operators.

$g(i)(t)$ is selected as

$$g(i)(t) = -a_3 i^3(t) - a_2 i^2(t) - a_1 i(t) - a_0 \tag{24}$$

The thresholds r_j are selected as $r_j = 0.3j$ $(j = 1, 2, ...n)$. The weights p_j, q_j, and a_0, ..., a_3 in (17) and (24) can be found using the nonlinear least-square optimization toolbox in MATLAB. The identified results [9] are shown in Table 1.

Table 1. Coefficients of the ASPI model

Numbers	r_j	p_j	c_j	q_j	a_j
0	0	0.9002			0
1	0.3	0.8445	1.1	1.3809	0
2	0.6	0.4276	1.2	0	0.3106
3	0.9	1.4821	1.3	0	0.0417
4	1.2	0.6097	1.4	0	
5	1.5	1.3596	1.5	0	
6	1.8	1.2051	1.6	0	
7	2.1	1.0574	1.7	0	
8	2.4	0.2835	1.8	1.0056	
9	2.7	0.1636			

Step 2: Identification of the dynamic part to find ρ_0, ρ_1 and ρ_2.
The s domain expression between $U(s)$ and $X(s)$ in (15) is expressed as

$$G(s) = \frac{X(s)}{U(s)} = \frac{\rho_0}{s^3 + \rho_2 s^2 + \rho_1 s + \rho_0} \tag{25}$$

To facilitate the identification, $G(s)$ is further decomposed as

$$G(s) = \frac{\tau}{s+\tau} \cdot \frac{\omega_n^2}{s^2 + 2\xi\omega_n s + \omega_n^2} \tag{26}$$

The objective is to identify the parameters of τ, ξ, ω_n in (26). To this end, a frequency response (1 to 500 Hz) of the magnetostrictive-actuated dynamic system is obtained in Fig. 1 (after normalization) with a 16 Kg mechanical load.

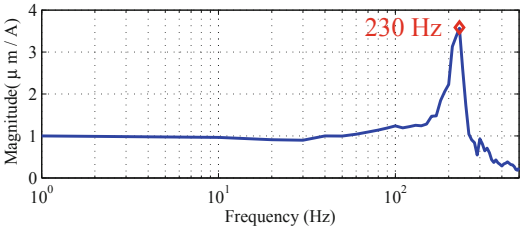

Fig. 1. Magnitude characteristics of the system

From the magnitude response in Fig. 1, we can find that $\omega_n = 230 \times 2\pi rad/s$. The other two parameters can also be determined as $\xi = 0.13$ and $\tau = 800 \times 2\pi$. Substituting these parameters in (26) yields

$$G(s) = \frac{1.05 \times 10^{10}}{s^3 + 5402s^2 + 3.98 \times 10^6 s + 1.05 \times 10^{10}} \tag{27}$$

Hence, ρ_0, ρ_1, and ρ_2 can be easily determined. The interested readers are referred to [9] for detailed identification procedure.

3.3 Controller Design with the Input Saturation

The control objective is to eliminate the hysteresis effect in the magnetostrictive actuator subject to the input saturation in order to improve the tracking performance of the positioning system. Towards this target, a backstepping control strategy combined with an anti-windup technique is developed. Figure 2 illustrates the control scheme.

Due to the existence of the hysteresis formulation in (16), the controller can not be directly designed. To achieve the controller design, the expression of the ASPI model considering the input saturation is reformulated as

$$u(t) = p_s sat_{\alpha,\beta}(i) - d(t) \tag{28}$$

where $p_s = p_0 + \sum_{j=1}^{n} p_j$, $d(t) \leq D_s$, and D_s is a constant. The detailed proof of the boundedness of $d(t)$ may refer to [9]. Define $b_p = \rho_0 p_s$ and $d_p(t) = \rho_0 d(t)$. The controller design is summarized in Table 2.

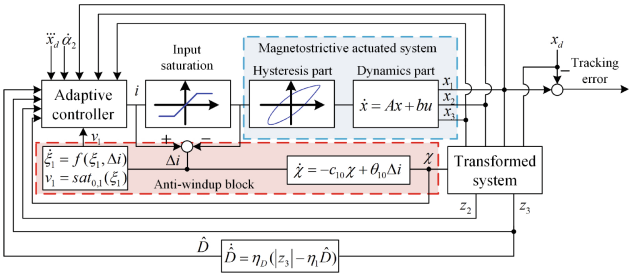

Fig. 2. The control diagram

Table 2. Adaptive backstepping control with anti-windup technique

Change of Coordinates:	
$z_1 = x_1 - x_d$	(T.1)
$z_2 = x_2 - \dot{x}_d - \alpha_1$	(T.2)
$z_3 = x_3 - \ddot{x}_d - \alpha_2 + \chi$	(T.3)
$\alpha_1 = -c_1 z_1$	(T.4)
$\alpha_2 = -c_2 z_2 + \dot{\alpha}_1 - z_1$	(T.5)
where c_1, c_2 are positive designed constants.	
Control Laws:	
$i(t) = \frac{1}{b_p}(-(c_3 - c_{30}v_1)z_3 - z_2 + \rho_2 x_3 + \rho_1 x_2 + \rho_0 x_1 - \hat{D}sgn(z_3) + \dddot{x}_d + \dot{\alpha}_2 + c_{10}\chi)$	(T.6)
$v_1 = sat_{0,1}(\xi_1)$	(T.7)
$\dot{\xi}_1 = sat_{-\rho^-,\rho^+}(c_L(sat_{0,\kappa}(c_L\lvert\Delta i\rvert) - \xi_1))$	(T.8)
$\dot{\chi} = -c_{10}\chi + \Delta i$	(T.9)
$\Delta i = i - sat_{\alpha,\beta}(i)$	
where $b_p = \rho_0 p_s$. c_{10}, c_L and θ_{10} are positive parameters.	
Parameter Update Law:	
$\dot{\hat{D}} = \eta_D(\lvert z_3\rvert - \eta_1\hat{D})$	(T.10)
where $\hat{D}$ is the estimation of D, with $D = \rho_0 D_s$.	
η_D, η_1 are positive designed constants.	

The stability of the closed-loop system is established in the following theorem.

Theorem 1. For the system (15) preceded by the ASPI model (17), the adaptive controller presented by (T.6)–(T.9) guarantees that the tracking error remains bounded.

Proof. From (15), and (T.1)–(T.5), we have

$$z_1\dot{z}_1 = z_1 z_2 - c_1 z_1^2 \tag{29}$$
$$z_2\dot{z}_2 = z_2 z_3 - c_2 z_2^2 - z_1 z_2 - \chi z_2 \tag{30}$$
$$\begin{aligned} z_3\dot{z}_3 = z_3(&-\rho_2 x_3 - \rho_1 x_2 - \rho_0 x_1 + b_p sat_{\alpha,\beta}(i(t)) \\ &-d_b(t) - \dot{\alpha}_2 - \dddot{x}_d + \dot{\chi}) \end{aligned} \tag{31}$$

where $d_p(t) = \rho_0 d(t)$.

Let $\tilde{D} = D - \hat{D}$. The Lyapunov function is constructed as follows

$$V(t) = \frac{1}{2}z_1^2 + \frac{1}{2}z_2^2 + \frac{1}{2}z_3^2 + \frac{1}{2\eta_D}\tilde{D}^2 + \frac{1}{2}\chi^2 \tag{32}$$

The time derivative of $V(t)$ along with (29)–(31) is given by

$$\begin{aligned} \dot{V}(t) = &-c_1 z_1^2 - c_2 z_2^2 + z_2 z_3 - \chi z_2 - \rho_2 x_3 z_3 - \rho_1 x_2 z_3 \\ &-\rho_0 x_1 z_3 + b_p i(t) z_3 - b_p \Delta i z_3 - d_b(t) z_3 - \dot{\alpha}_2 z_3 \\ &-\dddot{x}_d z_3 + \dot{\chi} z_3 + \frac{1}{\eta_D}\tilde{D}\dot{\tilde{D}} + \chi\dot{\chi} \end{aligned} \tag{33}$$

Substituting the control law $i(t)$ (T.6) into (33), one has

$$\begin{aligned} \dot{V}(t) = &-c_1 z_1^2 - c_2 z_2^2 - (c_3 - c_{30}v_1) z_3^2 - \chi z_2 - b_p \Delta i z_3 \\ &-\hat{D} sgn(z_3) z_3 + c_{10}\chi z_3 - d_b(t) z_3 + \dot{\chi} z_3 + \frac{1}{\eta_D}\tilde{D}\dot{\tilde{D}} + \chi\dot{\chi} \end{aligned} \tag{34}$$

Considering the definition of v_1 in (T.7), it is obvious that $v_1 \leq 1$. Besides, according to $-d_b(t)z_3 \leq D|z_3|$ and (T.10), one has

$$-d_b(t)z_3 - \hat{D}sgn(z_3)z_3 + \frac{1}{\eta_D}\tilde{D}\dot{\tilde{D}} \leq \tilde{D}|z_3| + \frac{1}{\eta_D}\tilde{D}\dot{\tilde{D}} = \eta_1 \tilde{D}\hat{D} \tag{35}$$

Hence, the inequality of $\dot{V}(t)$ considering (35) and (T.9) can be written as

$$\begin{aligned} \dot{V}(t) \leq &-c_1 z_1^2 - c_2 z_2^2 - (c_3 - c_{30}) z_3^2 - b_p \Delta i z_3 \\ &-c_{10}\chi^2 + \theta_{10}\Delta i \chi + \theta_{10}\Delta i z_3 - \chi z_2 + \eta_1 \tilde{D}\hat{D} \end{aligned} \tag{36}$$

According to the Young's inequality, we have

$$(\theta_{10} - b_p)\Delta i z_3 \leq (\theta_{10} - b_p) z_3^2 + \sigma_0 \tag{37}$$
$$\theta_{10}\chi\Delta i \leq \theta_{10}\chi^2 + \sigma_1 \tag{38}$$
$$-\chi z_2 \leq \chi^2 + \frac{1}{4}z_2^2 \tag{39}$$
$$\eta_1 \tilde{D}\hat{D} \leq -\frac{\eta_1}{2}\tilde{D}^2 + \frac{\eta_1}{2}D^2 \tag{40}$$

where $\sigma_0 = \frac{1}{4}(\theta_{10} - b_p)\Delta i^2$, $\sigma_1 = \frac{1}{4}\theta_{10}\Delta i^2$.

Considering the preceding inequalities in (37)–(40), one has

$$\dot{V}(t) \leq -c_1 z_1^2 - (c_2 - \frac{1}{4})z_2^2 - (c_3 - c_{30} - \theta_{10} + b_p)z_3^2 \\ -\frac{\eta_1}{2}\tilde{D}^2 - (c_{10} - \theta_{10} - 1)\chi^2 + \sigma_2 \tag{41}$$

where $\sigma_2 = \sigma_0 + \sigma_1 + \frac{\eta_1}{2}D^2$. Then we have

$$\dot{V} \leq -2\lambda V + \sigma_2 \tag{42}$$

where $\lambda = \min\{c_1, c_2 - \frac{1}{4}, c_3 - c_{30} - \theta_{10} + b_p, \frac{\eta_1\eta_D}{2}, c_{10} - \theta_{10} - 1\}$. Integrating it over $[0, t]$, one has

$$V(t) \leq \frac{\sigma_2}{2\lambda} + (V(0) - \frac{\sigma_2}{2\lambda})e^{-2\lambda t} \tag{43}$$

It should be noted that for any $\gamma > 0$, the set $B_r = \{z, \chi, \tilde{D} : V(z, \chi, \tilde{D}) \leq \gamma\}$ is a compact set, and assuming $||\Delta i||$ has a maximum on the set B_r. Therefore, the inequality in (43) shows that z_1,z_2, z_3, $\tilde{D}$ and χ are bounded as $t \to \infty$. The proof has been finished.

4 Simulation Results

To validate the effectiveness of the developed control approach, the simulation is conducted via MATLAB/SIMULINK. The control objective is to force the system output to follow a desired signal $x_d = 10\sin(2\pi t)$. The parameters in the controller and adaptive laws are selected as $c_1 = 1500$, $c_2 = 2000$, $c_3 = 90000$, $c_{10} = 1000$, $c_{30} = 60000$, $-\rho^- = -10$, $\rho^+ = 10$, $c_L = 1000$, $\kappa = 10$, $\theta_{10} = 1000$, $\eta_D = 100$, $\eta_1 = 1000$. The initial values are selected as $x_1(0) = 1$, $x_2(0) = 0$, $x_3(0) = 0$, $\xi_1(0) = 0$, $\chi(0) = 0$, $\hat{D}(0) = 0$. The saturation threshold value in (28) are set as $\alpha = -1.7A$ and $\beta = 1.7A$.

To illustrate the effectiveness of the anti-windup block, the comparisons are made among the following three conditions

- unconstrained systems
- constrained systems without anti-windup block
- constrained systems with anti-windup block

Figure 3(a)–(d) represent the comparison results. In Fig. 3(a), in order to follow the desired signal, for the unconstraint case, the controller generates a large current spike (around $-9.4A$) at the beginning, see the green dashed line in Fig. 3(a), which may burn out the magnetostrictive actuator in the real application. If a saturation block is directly applied (the case of constrained systems without anti-windup block), severe oscillations between the upper bound ($1.7A$) and lower bound ($-1.7A$) occur in the controller output, also leading large tracking errors, see the blue dotted line in Fig. 3(a) and (b). In the case of constrained systems with anti-windup block, although at the beginning the control strategy shows a large tracking error, the tracking error then maintains within 4 % and

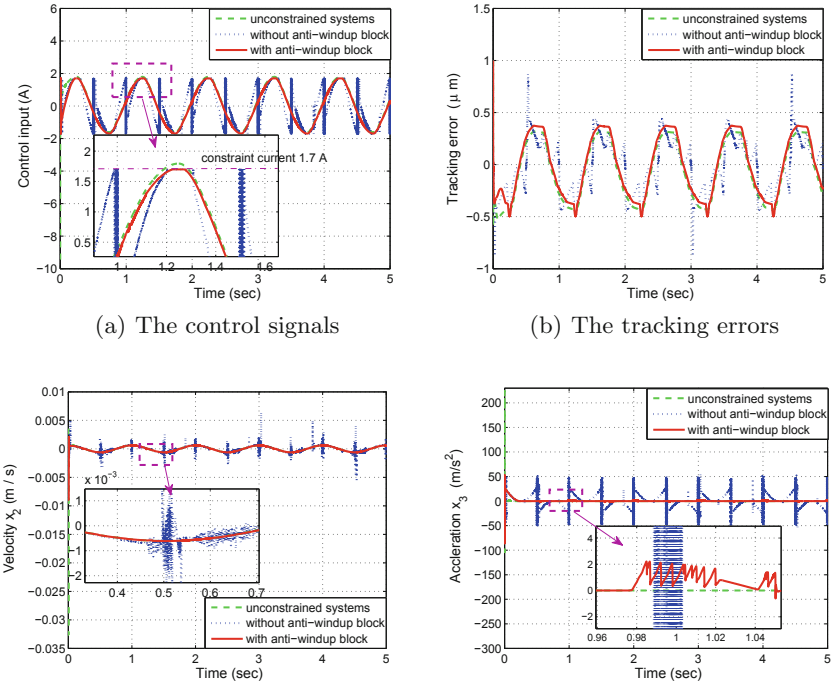

(a) The control signals (b) The tracking errors

(c) The velocity responses (d) The acceleration responses

Fig. 3. Simulation results with unconstrained systems, constrained systems without an anti-windup block and constrained systems with an anti-windup block (Color figure online)

no oscillations generated in the control signals, see the red solid line in Fig. 3(a) and (b). Figure 3(c) and (d) illustrate the comparisons of the velocity and acceleration at the end point of the magnetostrictive-actuated dynamic system. For the constrained system without the anti-windup block, the output of the actuator shows continuous oscillations, which might damage the actuator and reduce its lifespan. From above comparison results, it clearly demonstrates the effectiveness of the developed controller with the anti-windup block. For the future research, the output feedback control strategy combining the anti-windup block will be studied since in practical applications the velocity and acceleration of the actuator are not accessible.

5 Conclusion

Input saturation and hysteresis nonlinearity are two main problems that limit the performance of the magnetostrictive actuators. Towards these two problems, in this paper, an adaptive control approach combined with an anti-windup block is developed. From the simulation validation, the designed controller can effectively

suppress the oscillation caused by the input saturation meanwhile reducing the tracking error and hysteresis error to an acceptable range. In addition, the anti-windup block is independent of the adaptive controller, which is more feasible in practical implementation.

References

1. Li, Z., Su, C.-Y., Chai, T.: Compensation of hysteresis nonlinearity in magnetostrictive actuators with inverse multiplicative structure for preisach model. IEEE Trans. Autom. Sci. Eng. **11**(2), 613–619 (2014)
2. Gu, G., Zhu, L., Su, C.-Y.: Modeling and compensation of asymmetric hysteresis nonlinearity for piezoceramic actuators with a modified prandtl-ishlinskii model. IEEE Trans. Ind. Electron. **61**(3), 1583–1595 (2014)
3. Abidi, K., Sabanovic, A.: Sliding-mode control for high-precision motion of a piezostage. IEEE Trans. Ind. Electron. **54**(1), 629–637 (2007)
4. Shieh, H.-J., Hsu, C.-H.: An adaptive approximator-based backstepping control approach for piezoactuator-driven stages. IEEE Trans. Ind. Electron. **55**(4), 1729–1738 (2008)
5. Chen, M., Ge, S.: Adaptive neural output feedback control of uncertain nonlinear systems with unknown hysteresis using disturbance observer. IEEE Trans. Ind. Electron. **62**(12), 7706–7716 (2015)
6. Nikdel, N., Nikdel, P., Badamchizadeh, M.A., Hassanzadeh, I.: Using neural network model predictive control for controlling shape memory alloy-based manipulator. IEEE Trans. Ind. Electron. **61**(3), 1394–1401 (2014)
7. Teel, A.R., Zaccarian, L., Marcinkowski, J.J.: An anti-windup strategy for active vibration isolation systems. Control Eng. Pract. **14**(1), 17–27 (2006)
8. Sun, W., Zhao, Z., Gao, H.: Saturated adaptive robust control for active suspension systems. IEEE Trans. Ind. Electron. **60**(9), 3889–3896 (2013)
9. Li, Z.: Modeling and Control of Magnetostrictive-actuated Dynamic Systems. Ph.D. thesis, Concordia University, Canada, February 2015
10. Goldfarb, M., Celanovic, N.: Modeling piezoelectric stack actuators for control of micromanipulation. IEEE Control Syst. **17**(3), 69–79 (1997)
11. Adriaens, H., Koning, W., Banning, R.: Modeling piezoelectric actuators. IEEE/ASME Trans. Mechatron. **5**(4), 331–341 (2000)
12. Li, Z., Su, C.-Y., Chen, X.: Modeling and inverse adaptive control of asymmetric hysteresis systems with applications to magnetostrictive actuator. Control Eng. Pract. **33**, 148–160 (2014)